J Nanostruct 10(3): 564-580, Summer 2020

RESEARCH PAPER

Electrochemical and Microstructural Investigation of in-situ Grown CNTs Network on Carbon Paper as Electrocatalytic Electrode for Fuel Cells

Hajar Rajaei Litkohi [1*], *Ali Bahari*[2*] , *Reza Ojani*[3]

[1] *Department of Nanobiotechnology, Faculty of biotechnology, Amol University of Special Modern Technologies, Amol, Iran.*

[2] *Department of Physics, Faculty of basic sciences, University of Mazandaran, Babolsar, Iran.*

[3] *Department of Analytical Chemistry, Faculty of Chemistry, University of Mazandaran, Babolsar, Iran.*

ARTICLE INFO

Article History:
Received 12 February 2020
Accepted 29 April 2020
Published 01 July 2020

Keywords:
Carbon nanotubes
Catalytic support
Chemical vapor deposition
Fuel cell
Platinum
Wet impregnation

ABSTRACT

In this study, carbon nanotubes (CNTs) were deposited directly on impregnated Fe/carbon paper (CP) substrate (CNT/CP) utilizing chemical vapor deposition (CVD) process with the aim of using them as electrocatalytic electrode. The influence of wet impregnation conditions and CVD growth parameters on the characteristics of CNTs was investigated. Field emission scanning electron microscopy (FESEM), Energy dispersive spectroscopy (EDS), Transmission electron microscopy (TEM) and Raman spectroscopy were applied to characterize nucleation, growth and morphology of CNTs on CP. Measurement of Contact angle (CA) determined 125.9 and 145.0 ºC for CP and CNT/CP that displayed an increase in water repellence and degree hydrophobicity of CNT/CP to 15% than CP. Electrochemical impedance spectroscopy (EIS) analysis indicated the reduction of electrode charge transfer resistance from 5000 ohm value from CNT/CP to ohm value for CP that shows the increment in electrical conductivity of CNTCP. Half-cell test analysis represented that the improvement of performance and the increase of power density to ~8 % for Pt/CNT/CP compared to commercial catalyst Pt/C/CP (20 wt%) even with about 42% less Pt loading, can be attributed to strong adhesion of in-situ CNTs to the CP and lower agglomeration of CNTs along with outstanding electrical and thermal conductivity of CNTs. The obtained results indicated that the proposed nanostructure serves as a promising candidate for many technological applications specially carbon nanotube-supported catalyst.

How to cite this article
Rajaei Litkohi H., Bahari A. , Ojani R. Electrochemical and Microstructural Investigation of in-situ Grown CNTs Network on Carbon Paper as Electrocatalytic Electrode for Fuel Cells. J Nanostruct, 2020; 10(3): 564-580. DOI: 10.22052/JNS.2020.03.012

INTRODUCTION

In recent years, development of nanotechnology in the field of Science and Technology, attempts has been performed in order to achieve materials with high functionality, excellent quality and long lifetime. Among all innovative nanomaterials, Carbon nanotubes (CNTs) have attracted a great deal of attention due to their unique geometric shape, large specific surface area, excellent mechanical and thermal properties, high electric conductivity, fascinating chemical stability and relatively high oxidation stability [1–3]. These unique characteristics have made them proper candidates for many potential applications in various fields. Nowadays, carbon nanotube-

* *Corresponding Author Email: h.rajaei@ausmt.ac.ir*
a.bahari@umz.ac.ir

supported catalyst have been extensively used as electrocatalytic electrodes in a wide range of applications including lithium ion batteries, super capacitors, field emission probes, electrochemical sensors, vacuum electronic devices and fuel cells [4–7]. For this purpose CNTs are predominantly grown on various substrates such as silicon wafer, alumina, stainless steel, nickel foam, glassy carbon, activated carbon, carbon cloth, carbon paper, etc [8–14]. In 2020, Peter et al. fabricated short Pt nanorods on CNTs which were deposited directly on carbon paper via plasma enhanced chemical vapor deposition (PECVD) and directly employed as cathodes for PEMFCs[15].

According to literature reports, two strategies are usually used to load CNTs on different substrates. In conventional method, CNTs are coated on substrates using techniques such as ink process or loading after being purified and functionalized with suitable solvents and additive agents [16]. In order to improve CNTs dispersion, ultrasonication, magnetic stirring and covalent or non-covalent chemical treatments using acids, surfactants or polymers and plasma treatment are often being used [17]. However, these pretreatments have negative effects on the structure and properties of CNTs and the content of employed CNTs is also very low [18]. On the other hand, in the alternative method, CNTs are grown directly on substrate using techniques such as chemical vapor deposition (CVD) process which is able to uniformly distribute nanotubes on the substrate without agglomeration compared to conventional methods [19–23]. In addition, in-situ grown CNTs have strong adhesion to the substrate which leads to higher durability to substrate and improves electron and thermal transport properties between CNTs and substrates [18]. According to Tang *et al*. [18] another advantage of using in-situ processes to grow CNTs lies in that the electronic pathways at the three-phase zone are ensured. Therefore, an enhancement in catalyst utilization is observed in comparison to the conventional ink-process fabrication method. Due to high stiffness, high tensile strength, low weight, high chemical resistance, high temperature tolerance and low thermal expansion, carbon paper, one of the carbon substrates, has been widely used as substrate to synthesize CNT for catalytic support [19, 24]. Although many researchers have studied the synthesis of CNTs using in-situ an ex-situ methods, however, given the challenges ahead of in-situ method, much more research is necessary. Li *et al*. determined the optimal growth conditions of CNT arrays on CP substrate using catalyst seed-impregnated CVD method in which a conductive CB layer was in close connection to CNT arrays and CP to reduce contact electrical resistance[25]. Li *et al*. synthesized multiwall carbon nanotubes (MWCNTs)/carbon fiber paper (CFP) composite using a CVD set up in which different metal catalysts such as Cu, Fe and Ni were used [19]. However, randomly oriented MWCNTs were obtained only on Ni particles. Xie *et al.* fabricated the in situ grown CNTs on carbon paper as a GDL by a plasma-enhanced chemical vapor deposition process. Fuel cells using CNT-based GDLs showed better performance compared with the GDLs which employ Vulcan carbon black. The data obtained from the vapor permeability and the fuel cell performance tests indicated that the water flooding can be reduced by applying CNT-based GDLs which was attributed to its suitable hydrophobicity and proper structure[26]. In most cases before nanotube growth, catalyst deposition on carbon substrates is performed using variety of methods including sputtering [18, 27], e-beam evaporation [28], spin coating [29] and electrodepositing [30] in which the presence of advanced facilities and equipment is necessary and inevitable. Therefore, these methods are time-consuming and costly in comparison to impregnation method.

In this study, we applied a simple method to deposit MWCNTs on CP surface (CNT/CP) using wet impregnation and chemical vapor deposition methods (without hydrogen gas) which are both simple, affordable and have potential capability for high scale production. It was specifically demonstrated that changing the effective parameters in wet impregnation method can proportionally optimize the deposition of catalyst particles and ultimately result in uniform growth of nanotubes. Effect of CVD parameters including reaction temperature, and reaction time on morphology and yield of CNTs were determined. Enhanced hydrophobicity and enhancement of electrochemical active surface and reduction of charge transfer resistance compared to bare carbon paper suggest that this optimized electrode can be used as a suitable catalytic support for many technological applications of electrocatalytic electrodes. Finally, CNT/CP electrode decorated with Pt catalyst (Pt/CNT/CP) was prepared with

Ethylene glycol reduction process. Electrochemical investigations of the Pt/CNT/CP electrode were performed using the half-cell testing analyzer.

MATERIALS AND METHODES

Carbon paper (TGP0120) and the commercial 10 wt.% Pt/C catalyst were purchased from Fuel Cells ETC. Iron nitrate salt powder ($Fe(NO_3)_3 9H_2O$), Chloroplatinic acid (40 wt.%), Sodium hydroxide (97%), Ethanol, Sulfuric acid (98%), Nitric acid (69%) and Ethylene glycol were supplied from Merck Company and used without further purification. Nafion 117 membrane and Nafion solution (5 wt.%) were obtained from Dopunt.

Treatment of carbon paper sheets

Carbon paper sheets are mainly suitable to be used as carbon electrodes or gas diffusion layers due to high mechanical strength and porous structure. The sheets are typically made of irregular carbon fibers with diameters of 8 to 10 micrometers, density of 0.45 gr cm^{-3} and porosity of 78%. In order to prepare suitable catalyst particles, the CP sheets were treated in order to attach carboxyl, carbonyl and hydroxyl functional groups on their surface using the following procedure. In the first method, CP was soaked in ethanol for 1 h, while in the second method the CP was refluxed in 7 molar (M) nitric acid at temperature of 120°C for 5 h. After refluxing, the sheets were washed repeatedly by deionized water until pH reached about 5.

Synthesis of CNTs on CP support

Wet impregnation method was used for catalyst deposition due to simplicity, no need for advanced equipment or sophisticated materials, cost-effectiveness and time saving in comparison to other methods [25-29]. To prepare 0.3 M iron (III) catalyst solution, required amount of iron nitrate salt was dissolved in ethanol and ultra-sonicated for 20 min to reach a better dispersion. The CP pieces with 1cm ×1cm dimensions were impregnated in catalyst solution for periods of 1, 30, 60 and 120 min at room temperature so that catalyst ions can react with surface functional groups using ion adsorption process [31]. After washing and drying, samples were placed inside the CVD furnace, composed of a quartz tube with an internal diameter of 50 mm and a length of 120 cm with heating zone of 5 cm, for calcination and synthesis of CNTs. Initially, in order to calcination of samples and provide better adhesion of metallic iron and iron oxides particles to carbon fiber substrate, Ar gas (with 99.99% purity) was introduced with rate of 200 sccm (standard cubic centimeters per minute) at 500°C for 1 h. The temperature of the furnace was increased under constant Ar flow to the desired reaction temperatures (750, 800 and 850°C). In order to synthesize CNTs, acetylene gas (with 99.9% purity) was used as carbon supply because of its low decomposition temperature and cost effectiveness [32]. After calcination and raising the furnace temperature to the desired temperature, the required values of acetylene and Ar gases (Ar/C_2H_2: 10) flowed into the furnace and on the CP surface. When, the required time passed for nucleation and synthesis of CNTs (10, 15, 20, 30 min), the flow of acetylene gas was stopped and the furnace was turned off. Samples remained in the furnace under Ar flow rate of 300 sccm to reach ambient temperature. Schematic diagram of the whole CNTs synthesis process is shown in Fig 1.

Preparation of Pt/CNT/CP electrode for the half cell testing

In order to compare the performance of in-situ CNTs synthesized on carbon papers with the carbon black as commercial supporting catalyst layer for fuel cell cathode, the CNT/CP pieces were decorated with Pt catalyst using an ethylene glycol reduction method. First, the CNT/CP was refluxed in 5 M nitric acid at 120 ºC for 3 h and dried at 120 ºC for 5 h after washing several times with distilled water. Then refluxed CNT/CPs were immersed in desired amounts of catalyst solution which were previously dissolved in 25 mL of ethylene glycol and was stirred for 30 min. Few drops of 0.4 M NaOH were added until pH reached 9 and further stirred for 3 h at 120 ºC to complete the reduction process. After reaching room temperature, samples were washed and dried at 120ºC for 5h, named as Pt/CNT/CP. For comparison, the commercial 10 wt% Pt/C was sonicated with 2 mL ethanol and 10 µL of 5 wt% Nafion for 20 min. The slurry of Pt/C was loaded on CP, dried at 120ºC for 5 h, named as Pt/C/CP.

In order to prepare the working electrode for half-cell testing system, the processed Nafion membrane was soaked in 3 wt.% hydrogen peroxide and 0.5 M sulfuric acid at 80ºC for 2h (Liu et al. 2015). The prepared electrodes (Pt/CNT/CP or Pt/C/CP) and Nafion membrane were hot pressed at 1000 psi and 93 ºC after adding 20 µL of

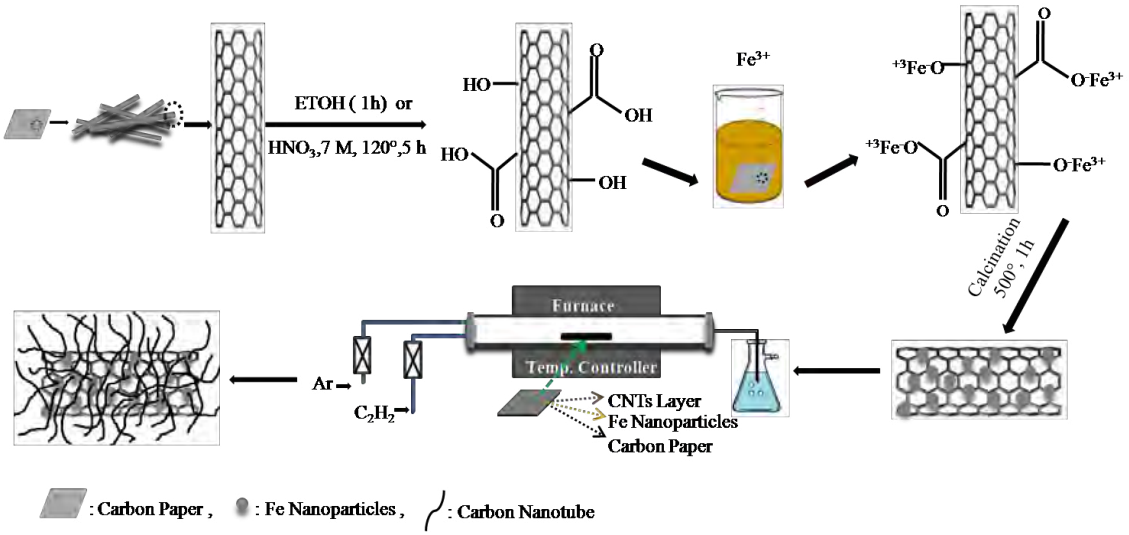

Fig. 1. Schematic diagram of the procedure to prepare in-situ grown CNTs on impregnated Fe/carbon paper.

5 wt.% Nafion solution. To obtain similar situations to that of polymer fuel cells, 0.5 M acid sulfuric electrolyte in contact with Nafion membrane and water trapped oxygen gas with flow rate of 0.2 bar was applied in contact with the catalyst layer.

Characterization techniques

The morphologies of CNTs/CP after Fe nanoparticles deposition and synthesis of CNTs were examined using a Field Emission Scanning Electron Microscopy (FESEM, Model: MIRA3-TESCAN) operated at voltage of 5 kV, equipped by an Energy Dispersive X-ray Spectroscopy (EDS: SAMx company, France) with an accelerating voltage of 5 kV. Transmission Electron Microscopy (TEM) images were recorded with a Zeiss-EM10C apparatus with an accelerating voltage of 80 kV. To prepare samples for TEM analysis, each piece of the carbon paper was soaked in deionized water and sonicated using a Misonix- S3000 ultrasonicator for 10 min. Then a drop of the solution was deposited on a carbon coated grid (Cu Mesh 300). Raman spectroscopy was performed on an Almega Thermo Nicolet Dispersive Raman Spectrometer with second harmonic 532 nm Nd:YLF laser excitation source in order to reveal the quality of CNTs in the papers. The laser was focused on a 100 µm spot size in the sample with power of less than 1 mW in order to keep the samples safe and prevent thermal degradation. The spectrum was measured over the range of 1000 to 2800 cm^{-1} with steps of 4 cm^{-1}. The contact angle (CA) of water droplets was measured using a CCD camera, OCA 15 plus, Dataphysics company with photography capability of Droplet. The electrochemical measurements were carried out at room temperature (23±1°C) using a potentiostat/galvanostat Ivium, 5612 AJ Eindhoven, Netherlands in a three electrode, two compartment configuration cell. A Platinum wire served as the counter electrode, a saturated calomel electrode (SCE) as the reference electrode and each piece of CP with 1cm×1cm dimensions as working electrode. The Fe loading on carbon paper was determined by inductively coupled plasma-optical emission spectroscopy (ICP-OES, Vista-Pro and Varian Australia). A SP150-Biologic potentiostat /galvanostat, was applied for half-cell test analysis. The counter electrode was a platinum wire, the reference electrode was Ag/AgCl and the working electrodes were 19 cm diameter circles of carbon substrate with contact surface area of 0.785 cm^2.

RESULTS AND DISCUSSION

In order to determine the relative effect of impregnation and CVD growth conditions on the CNTs/CP assembly, impregnation time, growth time and temperature were varied accordingly. The ratio of carbon source/carrier gas flow rate was also adjusted [33, 34]. The effect of these variations on the morphology and relative density of CNTs and electrochemical properties of CNTs/CP were quantified using FESEM, TEM, Raman spectroscopy, CA and CV analysis. The ethylene glycol process was applied to decorate the as

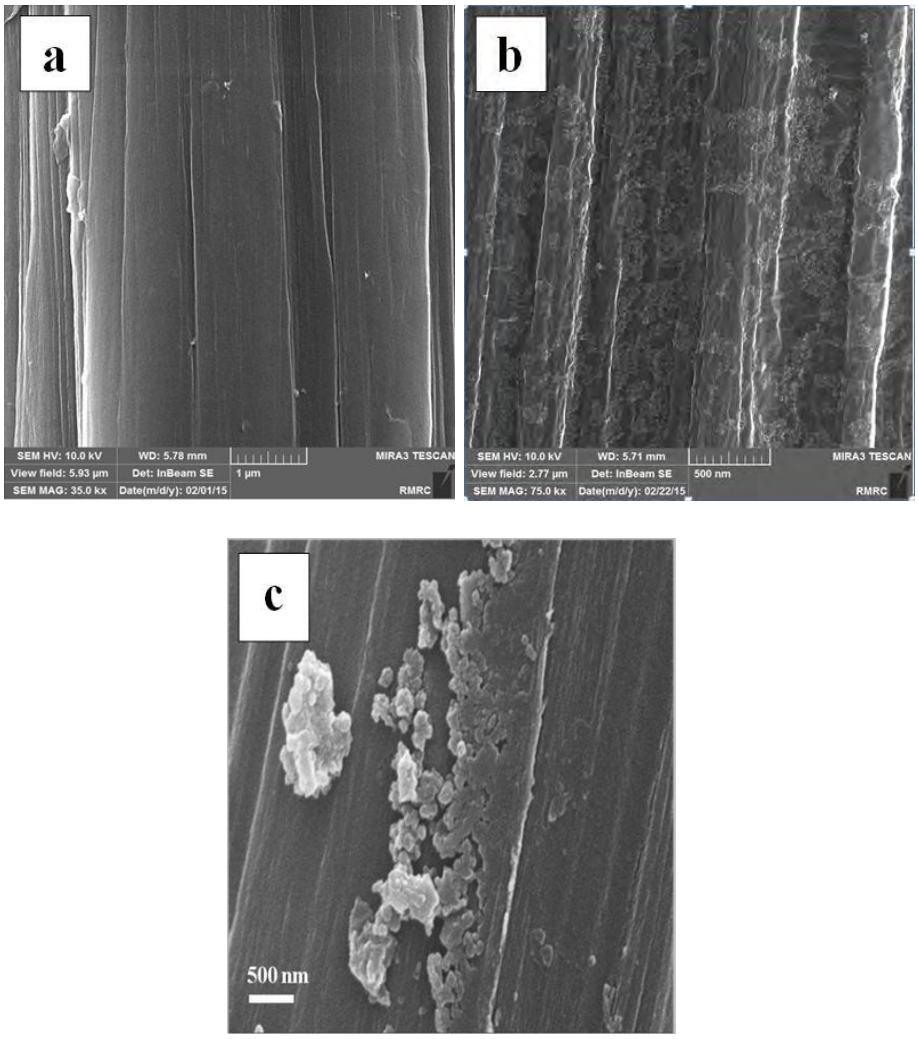

Fig. 2. FESEM images of (a) pristine carbon paper and impregnated carbon paper in 0.3 M Fe^{+3} solution catalyst loadings and pretreated in (b) ethanol and (c) nitric acid.

grown CNTs with Pt catalyst and the final electrode performance was examined by half-cell test.

Effect of pre-treating process on catalyst deposited CP

In order to investigate the deposition of catalyst particles on CPs, FESEM images were obtained. The CPs treated with ethanol, nitric acid and impregnated in solution of 0.3 M Fe^{+3} for 1 h, assigned as Fe/EtOH-CP and Fe/HNO_3-CP. Fig. 2 illustrates FESEM images of bare CP and impregnated CP in solution of 0.3 M Fe^{+3} for 1 h that was already treated in ethanol or refluxed in nitric acid. The images represent completely homogeneous deposition of catalyst nanoparticles on ethanol pretreated CP while the distribution and size of catalyst particles deposited on nitric acid refluxed CP is not uniform. In Fig. 2b uniform distribution of Fe particles on ethanol pretreated CP can be seen with dimension of 20 to 30 nm that were grown together to form a cluster or island. FESEM images specified that preparation or treatment of CPs with ethanol leads to homogeneous distribution of size and dispersion of catalyst nanoparticles on the CPs in comparison to nitric acid refluxed CPs. Certainly, this uniform distribution will affect the favorable growth of CNTs on the CP sheets.

Treatment of CP using ethanol solution introduces OH functional groups on the surface of CP while in nitric acid treatment apart from OH and COOH functional groups generation, carbon fiber walls in CP surface may be destroyed. Probably, destruction of carbon fibers walls, along

Table 1. Optimul conditions of different effective parameters of CNTs growth on carbon paperby CVD.

Parameters	Impregnation Time (min)				Growth Temperature (°C)			Growth Time (min)		
Ranges	5	30	60	120	750	800	850	10	20	30
Optimul Value			60			800			20	

with increasing functional groups can enhance the deposition of Fe particles on CP surface. The increase in catalyst loading, obtained from ICP analysis (as seen in Table 1), on Fe/HNO_3-CP compared to Fe/EtOH-CP shows that enhancement of deposited catalyst particles results in their agglomeration. Therefore, CP pretreated with ethanol for 1 h was chosen for the following experiments.

Also, to clarify nature and possible states of catalyst prepared by impregnation method, the XRD measurement was carried out. But there is not any diffraction peak representing the catalyst in the XRD pattern which is actually related to the low catalysts weight percentage generated through impregnation method [19, 35, 36]. This low loading was confirmed by ICP and EDS results, 1.9 wt% and 2.22 wt% respectively (illustrated in section 3.6).

Effect of catalyst impregnation time

In order to investigate the effect of impregnation time on the amount of catalyst particles and the nucleation of CNTs, the pretreated carbon papers were impregnated in catalyst solution for 5, 30, 60 and 120 min. After calcination and reaching the temperature of 800°C, argon and acetylene gas were simultaneously flowed for 5 min with flow rates of 150 sccm and 15 sccm, respectively. FESEM images of the samples were obtained after calcination and after the synthesis of CNTs, no significant difference in the samples was observed after calcination. Fig. 3 shows two different magnification FESEM images of the samples after synthesis process with increasing impregnation time. The remarkable point is the uniform growth of seedlings on the surface of all samples; it is obvious that an increase in impregnation time leads to increasing in the number of seedling. For the sample with 5 min impregnation time, the number of seedling was very limited while in the sample with 30 min impregnation time, the number of seedling was slightly increased (as seen in Figs. 3 a-d). Comparing Figs. 3e and g (samples with impregnation times of 60 and 120 min) shows that the excessive time of impregnation results in seedling over growth which further leads to the formation of agglomerated CNTs. Therefore, in the following investigations, all samples were impregnated in the desired catalyst solution for 1 h.

Effect of reaction temperature

After determination of the catalyst loading, further optimization experiments were performed by investigating the effect of reaction temperature for CNT growth. In order to optimize the reaction temperature, a series of growth processes were carried out at 750, 800 and 850°C with synthesis times of 20 min, the corresponding FESEM images of samples are illustrated in Fig. 4. In the sample under 750°C (Fig. 4a), no growth of CNTs was seen and only the nucleation of CNTs was formed which indicates that, at this temperature, decomposition of acetylene gas did not occur or can be attributed to the low solubility of carbon in iron catalyst at lower temperatures in comparison to the carbon-iron eutectic temperature [34]. According to Fig. 4b, increasing reaction temperature from 750 to 800°C resulted in substantial increase in the density of CNTs on the CP surface. As shown in Fig. 4c, further increase in reaction temperature from 800 to 850°C not only changed the morphology of tubular structures, but also increased their diameter. The diameters of CNTs were about 70 and 150 nm for 800, 850 °C, respectively. It can be due to the fact that with increasing temperature and sintering catalyst nanoparticles, the dimensions of catalyst particles increases, which in turn leads to an increase in diameter of deposited structures on the CPs [37]. Therefore, as discussed above, reaction temperature is one of the important factors to control of the density and morphology of CNT growth via the CVD process. Hence the action temperature was fixed at 800°C throughout the following experiment as the optimized temperature.

Effect of CNT growth time

According to CNTs growth mechanism, the density and morphology of CNTs on carbon paper could be influenced by the growth duration which is known to be an important factor for effective CNT growth [34]. Fig. 5 displays FESEM images of in-situ grown CNTs on CP samples that have been grown at different growth times of 10, 15, 20 and 30 min. Fig. 6a indicates that perfectly uniform nucleation and growth of CNT in all sample surface appeared after 10 min. It can be clearly seen that the diameter, length and density of the in-situ grown CNTs increased with growth time from 10 min to 20 min whereas such increase was not

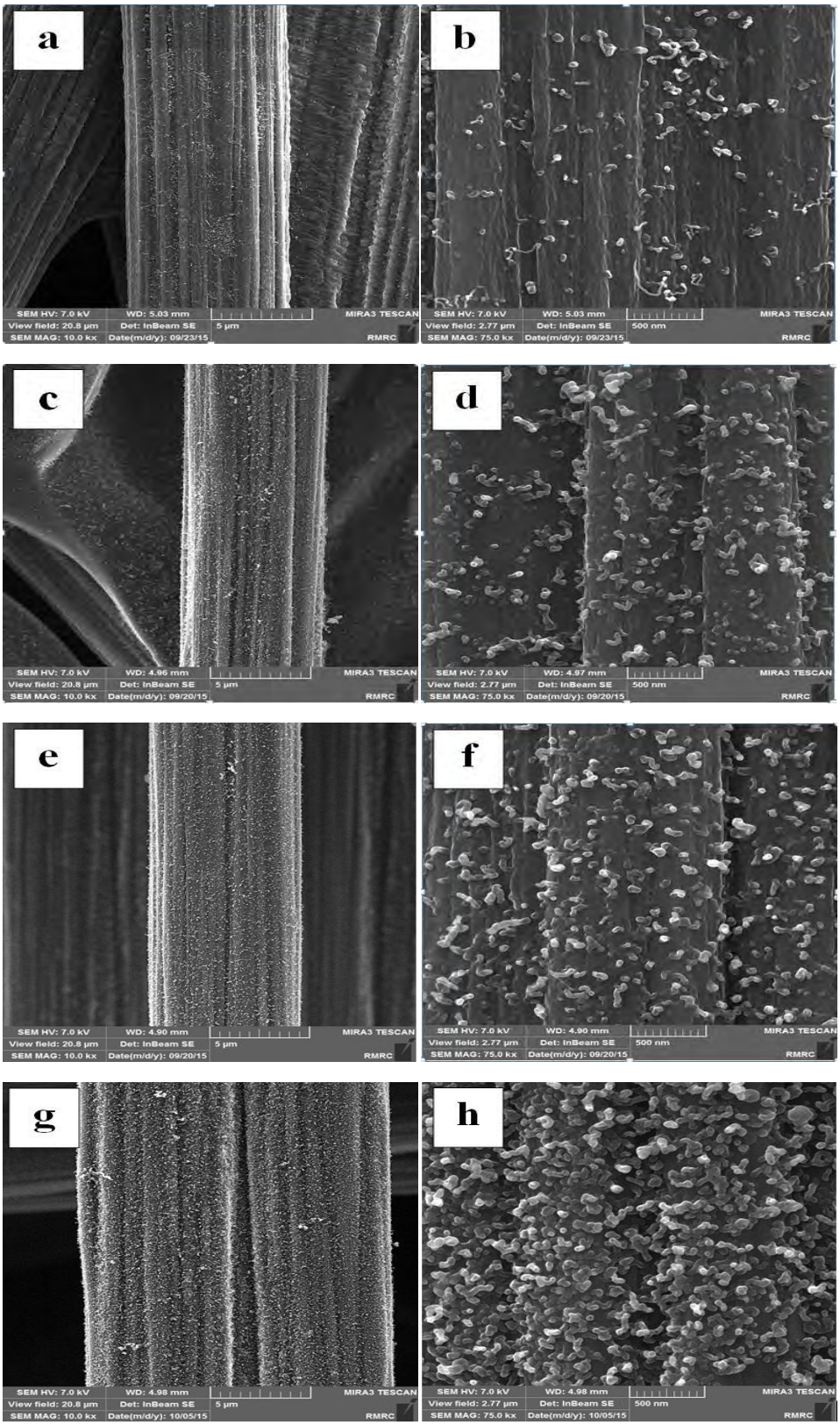

Fig. 3. Different magnification FESEM images of CNTs nucleation on carbon paper at 0.3 M Fe^{+3} solution with different catalysts impregnation times of: (a,b) 5min, (c,d) 30 min, (e,f) 60 min and (g,h) 120 min. Reaction temperature: 800°C; growth duration: 5 min; Ar/C_2H_2 flow rate: 150/15 sccm.

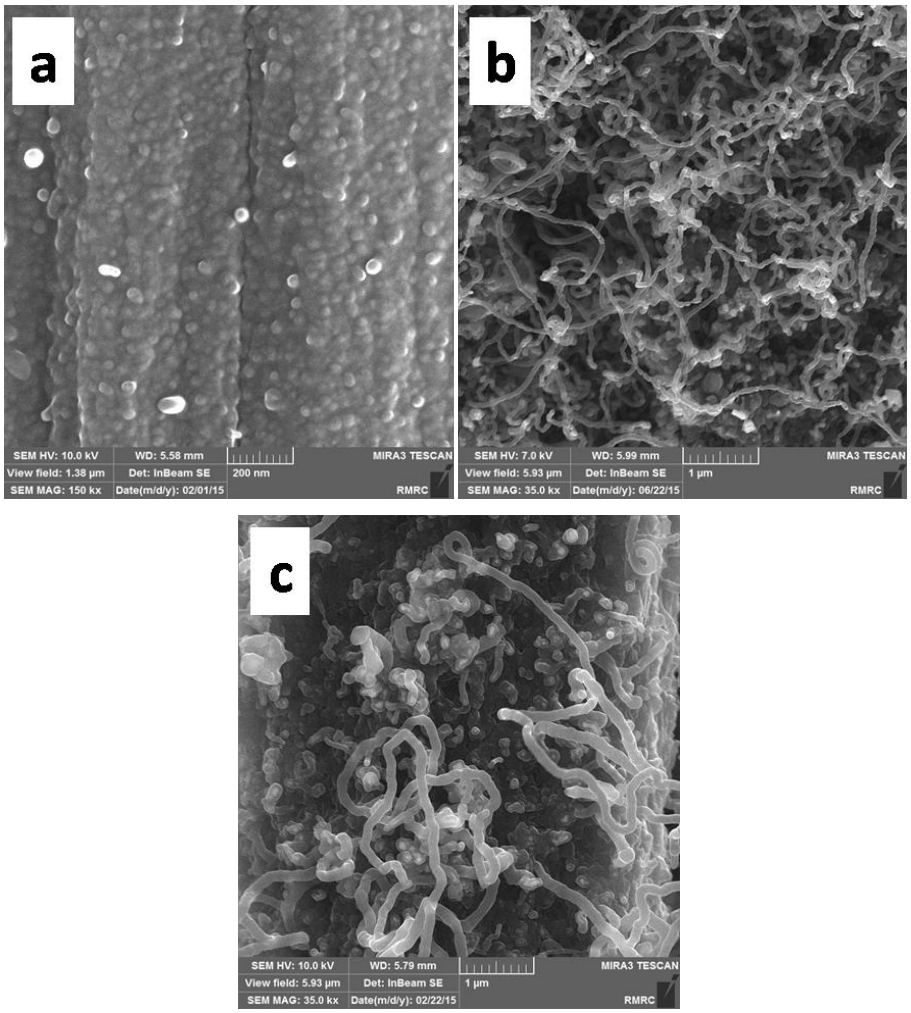

Fig. 4. FESEM images of CNTs directly grown on carbon paper at different reaction temperatures of: (a) 750 °C (b) 800°C and (c) 850°C. Fe^{+3} solution loading: 0.3 M; impregnation time: 1 h; growth duration: 20 min; Ar/C_2H_2 flow rate: 150/15 sccm.

observed when the growth time was further raised to 30 min. As shown in Figs. 6a and b, at growth times of 10 and 15 min, almost randomly oriented nanotubes were formed with approximate lengths of 150 nm and 1µm but when growth time reached 20 min, length of the CNTs was more than 5 micrometers with curved and tangled structures. When the growth time increased up to 30 min (Fig. 5c), it can be observed that in addition to the growth of CNTs a lot of impurities are abundantly grown.

Based on obtained optimal conditions are highlighted in Table 1 and considering the examined factors affecting in situ growth of CNTs on CPs and, a piece of CP was impregnated with 0.3 M Fe^{3+} catalyst solution for 1 h. Then after 1 h calcination at 500°C and reaching 800°C, the sample was exposed to Ar and C_2H_2 gases for 20 min with flow rates of 150 and 15 sccm, respectively. Figs. 6 display EDS spectra and FESEM images of the final sample at different magnifications. As Fig. 7 shows, not only an appropriate longitudinal growth of CNTs has been made, but also a very small amount of carbon impurities can be seen in the image. In fact, a network of CNTs was grown on the carbon fibers which cover over and between the fibers.

The elemental analysis of impregnated CPs in solution of 0.3 M Fe^{3+} before and after growth of CNTs for final sample was analyzed using EDS spectroscopy and illustrated in Table 2. Based on data from Table 2, 2.22 wt.% of Fe nanoparticles grow on the CP after wet impregnation which is almost the same as the value calculated from ICP analysis (1.9 wt.%). Also comparing the data in Table 2 reveals that the carbon percent increased

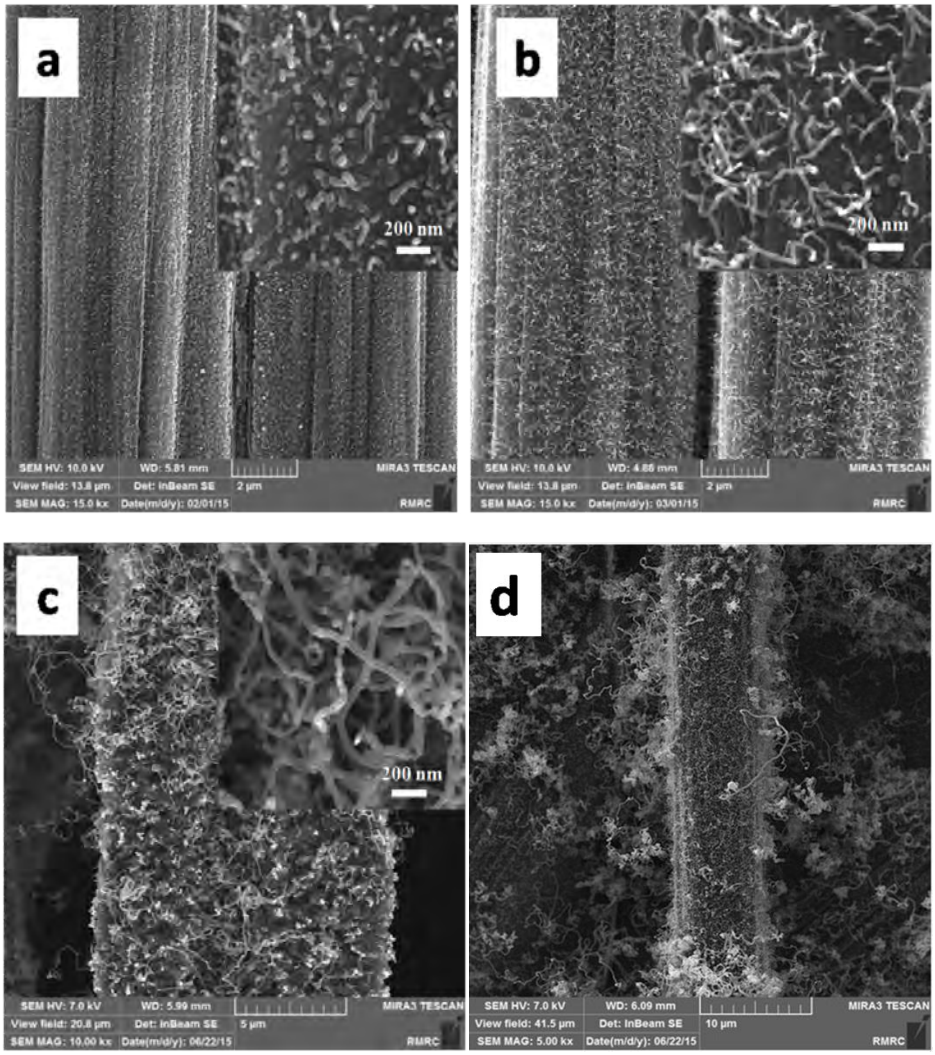

Fig. 5. FESEM images of CNTs directly grown on carbon paper at different growth durations: (a)10 min, (b) 15 min, (c) 20 min and (d) 30 min. Fe^{+3} solution loading: 0.3 M; impregnation time: 1 h; reaction temperature: 800°C; Ar/C_2H_2 flow rate: 150/15 sccm. (Inset: images with larger magnification)

from 87.5 wt% before CNTs growth to 93.18 wt% after CNTs growth with 6 wt% increase which is referred to as the yields of nanotubes.

Fig. 7 represents typical TEM images of CNTs directly grown on CP fibers synthesized using under different conditions. As shown in Fig. 7, the in-situ grown CNTs are multiwall and carbon impurities such as helical structures were grown before optimizing of the synthesis condition. However, the amounts of impurities reduced when optimum conditions of CNTs growth were attained. Fig. 7b displays an image of the final sample that specifies a multiwall carbon nanotube with diameter of 60 nm and length of about 5 µm.

As the ultimate goal of growing CNTs on CP substrate is to create a suitable support for the catalyst layer in electrocatalytic electrodes, it is predicted that the formation of interconnected network of CNTs has favorable effect on the growth of final catalysts such as Platinum on the CP substrate. In other words:

1. Growth of CNTs on carbon fibers with diameters much smaller than carbon fibers provides the possibility of growing final catalyst with lower size distribution.

2. Formation of a network of CNTs covering the space between the fibers provide more surface area for the growth of the final catalyst and as a result most of the spent catalyst such as platinum

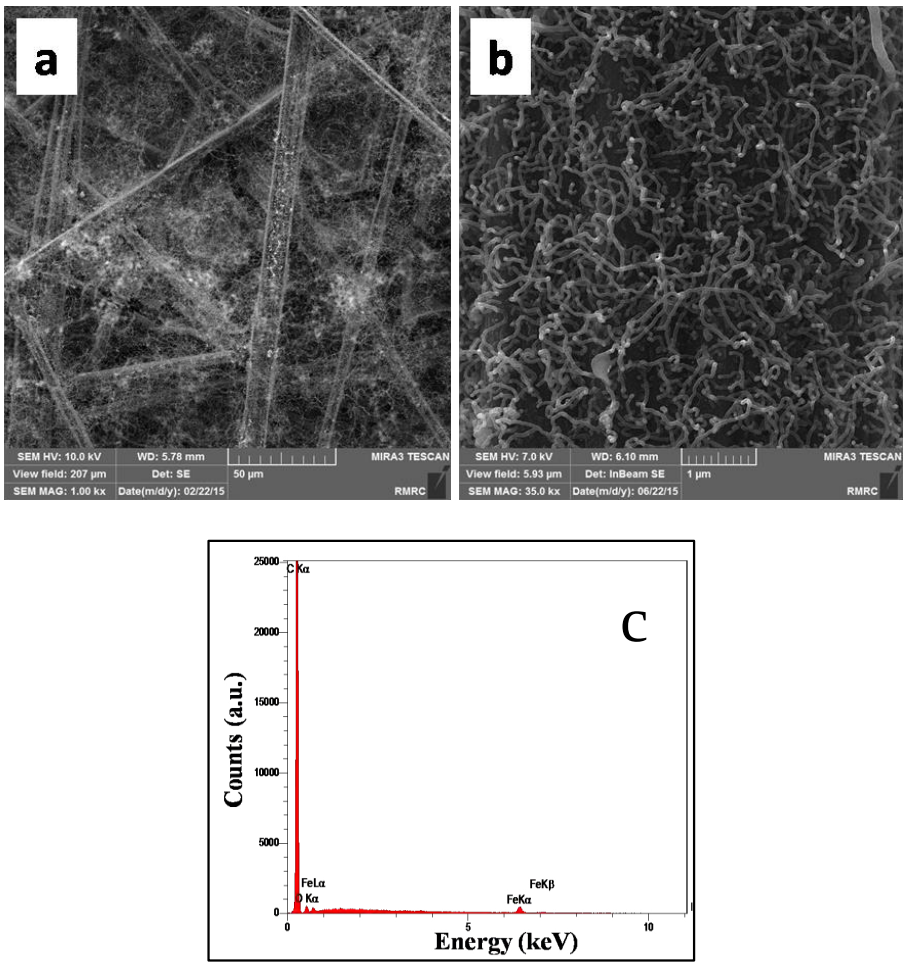

Fig. 6. FESEM images with different magnification and EDS spectra of CNTs directly grown on carbon paper at optimal conditions. Fe^{+3}solution loading: 0.3 M; impregnation time: 1 h; reaction temperature: 800°C; growth duration: 20 min Ar/C_2H_2 flow rate: 150/15 sccm.

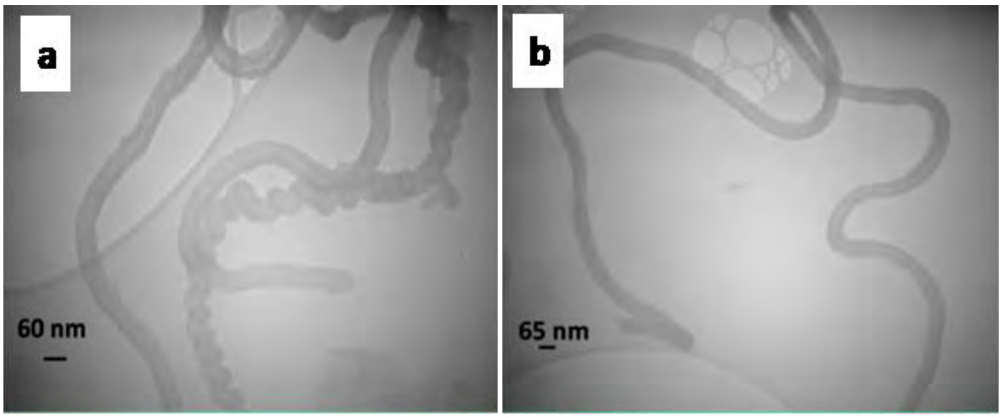

Fig. 7. TEM images of CNTs directly grown on carbon paper (a) before and (b) after optimum growth conditions.

Table 2. Quantitative results of impregnated CP in 0.3 M Fe^{+3}solution before and after CNTs growth by EDS analysis.

Element	before CNTs growth			after CNTs growth		
	Line	wt.%	at%	Line	wt.%	at%
Carbon	Ka	87.54	91.47	Ka	93.18	95.99
Oxygen	Ka	10.24	8.03	Ka	4.52	3.50
Iron	Ka	2.22	0.50	Ka	2.29	0.51

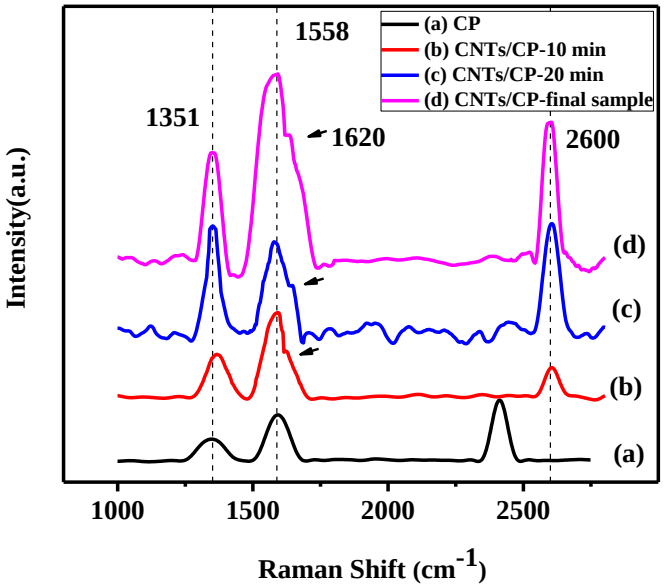

Fig. 8. Raman spectra of (a) bare CP, (b) CNTs/CP with growth duration of 10 min, (c) CNTs/CP with growth duration of 20 min and (d) CNTs/CP grown at optimized growth conditions (the final sample).

Table 3. Detailed information of Raman resonance variations in CP and as-grown CNTs on CP.

Sample Name	D band position (cm^{-1})	G band position (cm^{-1})	D' band position (cm^{-1})	2D band position (cm^{-1})	I_D/I_G (Height)	I_{2D}/I_D (Height)	FWHM (D band)
CP	1348	1592	----	2410	0.63	1.91	111.93
CNTs/CP-10 min	1366	1592	1621	2605	0.61	0.79	90.56
CNTs/CP-20 min	1351	1578	1625	2605	1.09	1.01	52.17

can be used at catalyst formation step. Thus, it is expected that catalysts with lower dimensions can be formed which in turn lowers catalyst consumption and as a result dramatically reduces the overall costs of any electrocatalytic electrode.

Raman Spectroscopy

Raman spectroscopy is a capable technique to detecting minor structural changes, which makes it a very valuable tool in the characterization of carbon materials[38, 39]. In Fig. 8, Raman spectrum of bare CP is compared to carbon nanostructures grown on CP via the CVD process. The Raman spectra of grown samples confirm again that the carbon deposits grown on the CPs are multiwall CNTs as was observed in TEM image. Detailed information of Raman resonance is summarized in Table 3. Whilst all spectra display D and G bands common to carbon based materials, there are notable differences in the all spectra which confirm the results obtained in microscopy images. The low intensity of D-band at 1351cm^{-1} for CP indicates high degree of graphitization in bare CP [40].

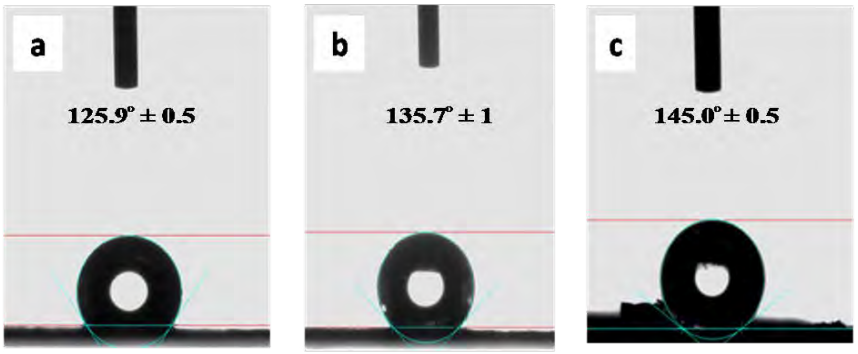

Fig. 9. Cross-sectional view photographs for water droplets on: (a) bare carbon paper and grown CNT directly grown on the CP with growth duration of (b) 10 min and (c) 20 min (for final sample).

The 2D-band appearing at 2400 cm^{-1} is assigned to the overtone of D-band which corresponds to the existence of order in a wide range of material arising from a second order of double phonon scattering process creating an elastic phonon. Fig. 8b shows the spectrum of sample prepared at growth time of 10 min with tube-like structures, length of less than 1 µm and diameter of about 20 to 30 nm. Intensity of both D and G bands are not much different compared to bare CP peaks due to the very low yields of products but sharper peaks represents the growth of CNTs. Figs. 8c and d show the spectrum of samples before and after the optimal growth conditions with different purities as seen in related FESEM images in Figs. 5c and 6. The intensity ratios of D/G and 2D/D bands are known as one of the important features to determine the graphitization degree or lattice distortion in carbon materials. As can be seen in Table 3, the decrease in ratio of I_D /I_G and increase in ratio of I_{2D} /I_D corresponds to fewer defects and higher quality of CNT structures. Another index of the relative graphitization in carbon based samples is the full width at half maximum (FWHM) intensity of the D-band [41]. As can be seen in spectrums, reduction of the amount of impurities results in decreasing FWHM of the D-band. A clear difference between Raman spectra of bare CP and CNTs is the appearance of D' shoulder in the region of 1617- 1625 cm^{-1} near the G-band. Appearance of this peak may be assigned to small crystallite sizes appearing when two-dimensional order is formed [40, 42].

Contact Angle results

Figs. 9 a-c show cross-view photographs of water droplet on the surface of bare carbon paper and in-situ grown CNTs with growth durations of 10 min and 20 min (the final sample), respectively. To indicate the hydrophobicity of the samples surface, three drops of water were put at different positions on a sample surface and the deviation of three contact angle readings was about 2.5°. According to the measurements, the Contact Angle of water droplet for bare carbon paper and samples grown at 10 and 20 min were 125.9, 135.7 and 145.0°, respectively. The CA measurements display that the wetting of CP was changed by growth of CNTs as the degree of hydrophobicity of CP was increased. Results indicated that the changes in the degree of hydrophobicity depend on the thickness of the CNTs network that grown on the CP. The hydrophobicity of the sample grown at 10 min with length of less than 1 µm increased 7.8% while the sample with growth duration of 20 min (the final sample) and length of more than 5 µm encountered 15% increase. This can be related to the formation of valleys and hills during the growth of CNTs on the CP surface which decreases the available surface contact area to water [43]. For CNTs, the hydrophobicity originated from the appearance of hydrophobic C=C or C–H groups which prevents permeation of water into the valleys [44], when water droplets are placed on the surface of CNTs network, a few air trapped into the created valleys and hills that in turn prevented the penetration of more water [45, 46]. Therefore, the water droplet forms a quasi-spherical shape on the CP surface and therefore could not be able to wet the substrate surface.

Electrochemical investigation

Voltammetry is a standard technique used for electrode characterization. Hence, the electrochemical properties of both CNTs/CP (for the optimized final sample) and bare CP electrodes were determined by Cyclic Voltammetry. Fig. 10 shows CVs of CNTs/CP electrode and bare CP

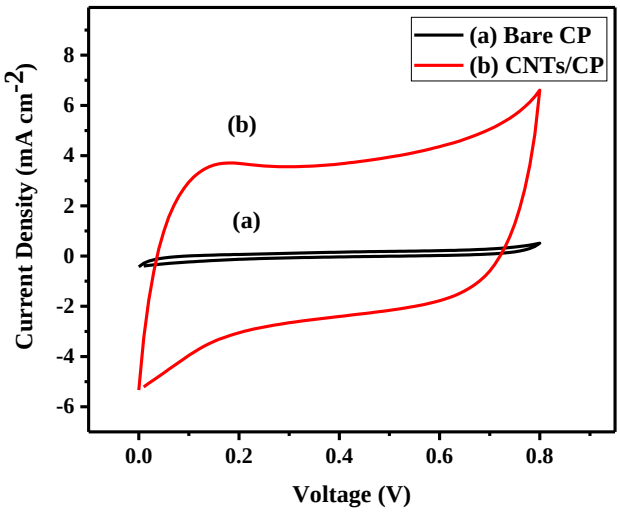

Fig. 10. Cyclic Voltammograms of (a) bare CP and (b) CNTs/CP grown at optimized growth conditions in 0.5 M H_2SO_4 at 10 mV s^{-1}.

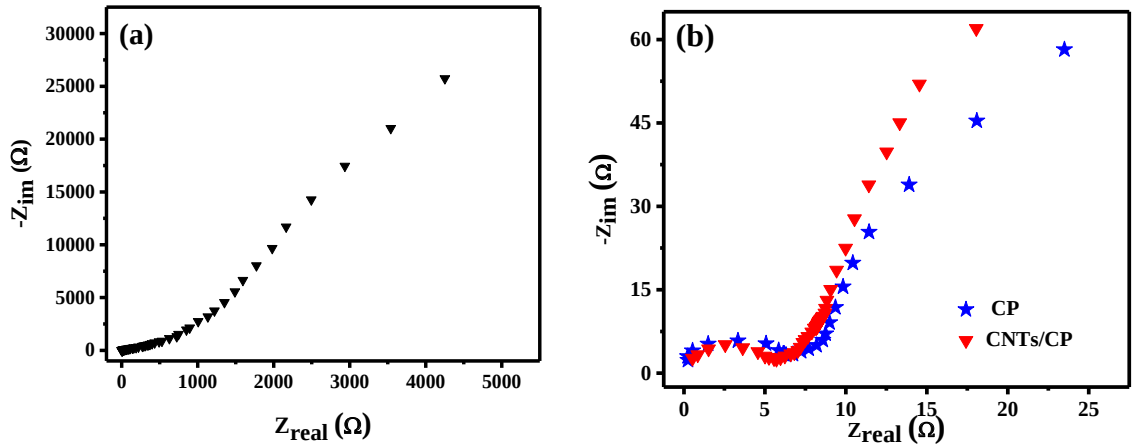

Fig. 11. Nyquist diagrams of (a) bare CP and (b) CNTs/CP grown at optimized growth condition (with the plot of CP electrode in low impedance range for comparition) in 0.5 M H_2SO_4 at the OCP potentials , (a): -0. 265V and (b): -0.771 V.

electrode in 0.5 M H_2SO_4 in order to examine whether CNTs were deposited on CP support. Comparing the two curves in Fig. 10 indicates that these MWCNTs are electrically connected to the CP of the fuel cell backing layer [47]. The form of rectangular shape of voltammetry characteristic of CNTs/CP electrode in Fig. 10 show the behavior similar to electric double layer capacitors (EDLC) [48]. The storage mechanism in EDLCs or ultracapacitors is not Faradic, but only it is based on ion adsorption between the interfaces of electrodes and electrolyte. Therefore, there is no chemical reactions on the charging and discharging of such ultracapacitors and the energy is stored electrostatically [49]. These electrodes are only based on carbon materials with large specific surface area, such as CNTs due to their highly accessible surface area, nano-scale structure and good electrical conductivity [50]. Comparing the curves in Fig. 11 specifics the higher charging and discharging capacitance for modified electrode by CNTs. This can be attributed to larger reaction surface area and easy transport of electrons from CNTs to CP that can be originated from either ballistic electron transport or high density of state in the CNTs [51].

Electrochemical impedance spectroscopy (EIS) was used to investigate the electrochemical behavior of the electrodes. The EIS spectra of CP and CNTs/CP electrodes were measured in the frequency range of 100 kHz to 0.1 Hz at open circuit potential. The typical Nyquist plots of CP and

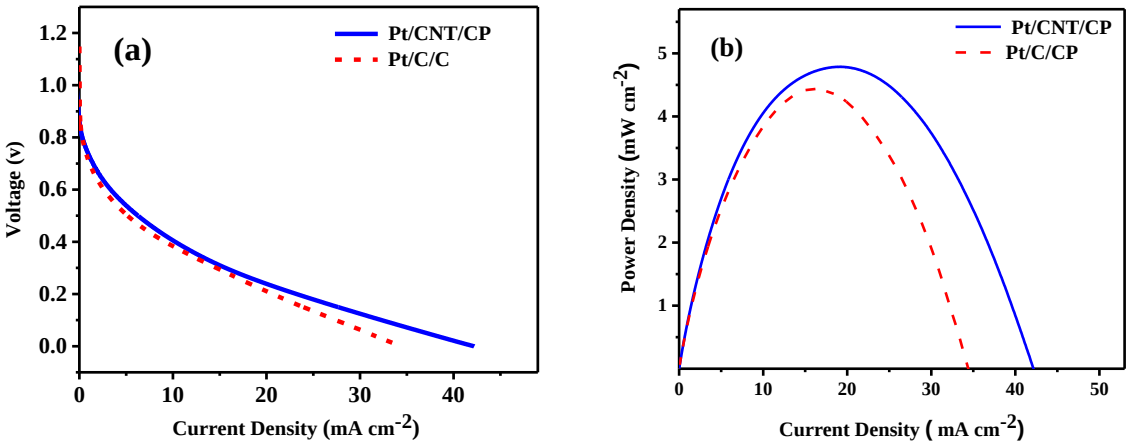

Fig. 12. The comparison of the half-cell test performance using the Pt/CNT/CP and Pt/C/CP electrodes: (a) Current–Potential curves and (b) Current–Power curves, in 0.5 M H_2SO_4 at the potential 0.4 V (vs SCE).

CNTs/CP electrodes present in Fig. 11a and b. Also, the Nyquist plot of CP electrode in low impedance range is shown in Fig. 11b for comparing the behavior of electrodes. The Nyquist plots consist of a semicircular curve in the high frequency region and an inclined line at low frequency. The high frequency semicircle corresponds to charge transfer resistance in which larger diameters of semi-circle indicates lower electrical conductivity [19]. As shown in Fig. 11b, the diameter of semi-circle CNTs/CP electrode is less than CP electrode that indicating the reduction of electrode charge transfer resistance. Also the impedance range of both curves is quite comparable, kilo-ohm impedance of CP electrode in comparison to ohm impedance of CNTs/CP electrode. The different range of electrodes impedance indicates the increment in electrical conductivity of the modified CNTs/CP electrode than pure CP electrode. Conductivity of CP electrode is relatively weak while high conductivity of CNTs/CP is related to the additional conductivity provided by the network of CNTs on the surface of CP. In addition, ultra-high electrical conductivity of CNTs can compensate the contact resistance between CNTs themselves and between CNTs and CP in CNTs/CP electrode. The inclined line at low frequency indicates a capacitor response that if the slope of line is near to 90°, it behaves like a ideal capacitor [52, 53]. Therefore EIS spectra of electrodes present the behavior similar to EDLC, as seen in Cyclic Voltammetry. The slope of linear part for CNTs/CP electrode is more than CP electrode that specifies the enhancement of charge/discharge capacitance for modified electrode by CNTs. Increasing of charging and discharging capacitance can be due to outstandig properties of CNTs such as high reaction surface area. CV and EIS results along with wonderful microstructure of composite reveal that the CNTs/CP composite is an appropriate choice as catalyst support or electrocatalytic electrode for many technological applications.

Also, the main issues for using CNTs in electrocatalytic electrodes are concerning the adhesion of these CNTs to the CP and subsequently ensuring the amount of remained CNTs on the CP during the following processes such as catalyst deposition and working electronic devices. In order to investigate the durability of CNTs on the CP, the final sample was immersed in deionized water and ultrasonicated for 1 h. As expected, after sonication there were no visible black particles in solution that indicates the CNTs adhered strongly to the CP due to their in situ-growth on Carbon paper support.

The performance of Pt/CNT/CP electrode at half-cell testing

Finally, the electrocatalytic performance of the Pt/CNT/CP electrode for PEM fuel cell cathode and comparison with commercial Pt/C coated CP were tested using a half-cell testing setup. The half-cell ex-situ setup provides a fast and highly cost-effective approach to investigate the cathode half reaction in polymer fuel cells, the related catalytic mechanism and the effect of operating conditions on the reaction for optimal selection of the catalyst and catalytic substrate. The potential ranges of 1.2 to 0 V with scan rate of 10 mV s^{-1} was applied to activate each electrode. Fig. 12 shows the recorded polarization and P-I curves of the Pt/CNT/CP, and Pt/C/CP electrodes. The details of the half-cell testing for the CP, CNT/CP and Pt/CP electrodes have been discussed in previous reports (Rajaei Litkohi et al. 2017). The maximum power density and the related current density and

Table 4 Maximum power density and related current density and voltage of the prepared electrodes and comparison to the reference electrodes.

Electrode	P_{max} (mW/cm^2)	I (mA/cm^2)	References
CP	0.125	0.718	Rajaei Litkohi et al. (2017)
CNT/CP	0.173	1.171	
Pt/CP	0.385	1.494	
Pt/C/CP	4.437	15.93	This study
Pt/CNT/CP	4.787	19.150	

voltage obtained from half-cell test for prepared electrodes and reference electrodes are presented in Table 4, as well. A comparison of maximum power density of Pt/CNT/CP, CNT/CP and CP indicates that catalyst plays animportant role in oxygen reduction reactions (ORRs) at the site of the cathode electrode of the fuel cell; the existing of CNTs without a catalyst (CNT/CP electrode) had no effect on the oxygen reduction reaction. The maximum power densities for the Pt/CNT/CP and Pt/C/CP were 4.787 and 4.437 mW/cm^2, at current densities of 19.150 and 15.930 mA/cm^2, respectively. Therefore, when the particles of the Pt catalyst are deposited on the CNT/CP electrode, the oxygen reduction reaction rate is reduced; its maximum power increases by about 8% from 4.787 to 4.437 mW/cm^2 compared to a platinum electrode coated on Carbon black/CP. For a more accurate comparison of the performance of the electrodes, an ICP analysis was performed to obtain the precise amount of Pt catalyst in the Pt/CNT/CP and Pt/C/CP electrodes. It was revealed that the amount of Pt catalyst in Pt/CNT/CP was 8.5 wt% which is much lower than the 20 wt% for Pt/C/CP. Thus, the Pt/CNT/CP electrode exhibits higher electrocatalytic performance in comparison to the Pt/C/CP electrode, despite lower Pt catalyst loading. The reason can be attributed to unique morphological structure and intrinsic electrical properties of the CNTs or fast electron transfer and less energy loss through direct growth of CNTs on carbon paper.

CONCLUSION

This work has demonstrated that the degree of hydrophobicity and electrochemical activity of CP including carbon fibers can be enhanced by decoration of CNTs. A CNTs/CP electrode was formed by catalytic growth of CNTs on CP using CVD technique. FESEM, TEM and Raman analysis showed that the parameters governing wet impregnation method and CVD growth have significant impact on the nucleation and growth of CNTs, which subsequently affects their structure and morphology. The synthesized CNTs/CP electrode under optimized conditions presents 15% water repellency enhancement compared to bare CP. It can be originated from hydrophobic characteristics of CNTs as well as a large amount of air trapped between CNTs network that prevents the wetting of CP. Also electrochemical characterizations showed the behaviour of electric double layer capacitor and reduction of charge transfer resistance of the CNTs/CP electrode compared to CP. In addition, the results of half-cell testing investigations demonstrated that the electrocatalytic performance and power density of Pt/CNT/CP is about 8% higher than Pt/C/CP electrode even with about 42% less Pt loading, which can be attributed to the increase in surface area, ballistic electron transport or high density of state in the CNTs compared with carbon black. Therefore, obtained results from CA, CV, EIS and half-cell testing characterizations suggest that the CNTs/CP composite can be considered as a promising candidate for many technological applications specially carbon nanotube-supported catalyst.

CONFLICT OF INTEREST

The authors declare that there are no conflicts of interest regarding the publication of this manuscript.

REFERENCES

1. Mardle P, Ji X, Wu J, Guan S, Dong H, Du S. Thin film electrodes from Pt nanorods supported on aligned N-CNTs for proton exchange membrane fuel cells. Applied Catalysis B: Environmental. 2020;260:118031.
2. Yarahmadii A, Rajabi M, Talafi Noghani M, et al. Synthesis of Aluminum- CNTs Composites Using Double-Pressing Double-Sintering Method (DPDS). J Nanostructures 2018; 0: 94–102.
3. Litkohi HR, Bahari A, Ojani R. Synthesis of Pt-Ni-Fe/CNT/CP nanocomposite as an electrocatalytic electrode for PEM fuel cell cathode. Journal of Nanoparticle Research. 2017;19(8).
4. Abnavi A, Faramarzi MS, Sanaee Z, et al. SnO2 Nanowires on Carbon Nanotube Film as a High Performance Anode Material for Flexible Li-ion Batteries. J Nanostructures 2018; 8: 288–29.
5. Alipour MoghadamEsfahani R, Vankova SK, Easton EB, Ebralidze II, Specchia S. A hybrid Pt/NbO/CNTs catalyst with high activity and durability for oxygen reduction reaction in PEMFC. Renewable Energy. 2020;154:913-24.
6. Li D, Cheng Y, Wang Y, Zhang H, Dong C, Li D. Improved field emission properties of carbon nanotubes grown on stainless steel substrate and its application in ionization

gauge. Applied Surface Science. 2016;365:10-8.
7. Thirumal V, Pandurangan A, Jayavel R, Krishnamoorthi SR, Ilangovan R. Synthesis of nitrogen doped coiled double walled carbon nanotubes by chemical vapor deposition method for supercapacitor applications. Current Applied Physics. 2016;16(8):816-25.
8. Litkohi HR, Bahari A, Ojani R. Synthesis of Pt-Ni-Fe/CNT/CP nanocomposite as an electrocatalytic electrode for PEM fuel cell cathode. Journal of Nanoparticle Research. 2017;19(8).
9. Hashempour M, Vicenzo A, Zhao F, Bestetti M. Direct growth of MWCNTs on 316 stainless steel by chemical vapor deposition: Effect of surface nano-features on CNT growth and structure. Carbon. 2013;63:330-47.
10. Wu J-Z, Li X-Y, Zhu Y-R, Yi T-F, Zhang J-H, Xie Y. Facile synthesis of MoO2/CNTs composites for high-performance supercapacitor electrodes. Ceramics International. 2016;42(7):9250-6.
11. Kamavaram V, Veedu V, Kannan AM. Synthesis and characterization of platinum nanoparticles on in situ grown carbon nanotubes based carbon paper for proton exchange membrane fuel cell cathode. Journal of Power Sources. 2009;188(1):51-6.
12. Gong Q-J, Li H-J, Wang X, Fu Q-G, Wang Z-w, Li K-Z. In situ catalytic growth of carbon nanotubes on the surface of carbon cloth. Composites Science and Technology. 2007;67(14):2986-9.
13. Hermas A-EA, Abdel Salam M, Al-Juaid SS. In situ electrochemical preparation of multi-walled carbon nanotubes/polyaniline composite on the stainless steel. Progress in Organic Coatings. 2013;76(12):1810-3.
14. Park SJ, Lee DG. Development of CNT-metal-filters by direct growth of carbon nanotubes. Current Applied Physics. 2006;6:e182-e6.
15. Mardle P, Ji X, Wu J, Guan S, Dong H, Du S. Thin film electrodes from Pt nanorods supported on aligned N-CNTs for proton exchange membrane fuel cells. Applied Catalysis B: Environmental. 2020;260:118031.
16. Nakagawa K, Yasumura Y, Thongprachan N, Sano N. Freeze-dried solid foams prepared from carbon nanotube aqueous suspension: Application to gas diffusion layers of a proton exchange membrane fuel cell. Chemical Engineering and Processing: Process Intensification. 2011;50(1):22-30.
17. Scheibe B, Borowiak-Palen E, Kalenczuk RJ. Oxidation and reduction of multiwalled carbon nanotubes — preparation and characterization. Materials Characterization. 2010;61(2):185-91.
18. Tang Z, Poh CK, Lee KK, Tian Z, Chua DHC, Lin J. Enhanced catalytic properties from platinum nanodots covered carbon nanotubes for proton-exchange membrane fuel cells. Journal of Power Sources. 2010;195(1):155-9.
19. Li Y-h, Gao H-q, Yang J-h, Gao W-l, Xiang J, Li Q-y. Multi-wall carbon nanotubes supported on carbon fiber paper synthesized by simple chemical vapor deposition. Materials Science and Engineering: B. 2014;187:113-9.
20. Hsieh C-T, Hung W-M, Chen W-Y. Electrochemical activity and stability of Pt catalysts on carbon nanotube/carbon paper composite electrodes. International Journal of Hydrogen Energy. 2010;35(16):8425-32.
21. Hashempour M, Vicenzo A, Zhao F, Bestetti M. Effects of CVD direct growth of carbon nanotubes and nanofibers on microstructure and electrochemical corrosion behavior of 316 stainless steel. Materials Characterization. 2014;92:64-76.
22. Shahi F, Pasha MA, Hosseini AA, et al. Synthesis of MWCNTs Using Monometallic and Bimetallic Combinations of Fe , Co and Ni Catalysts Supported on Nanometric SiC via TCVD. J Nanostructures 2015; 5: 87–95.
23. Ahangarpour A, Farbod M, Ghanbarzadeh A, et al. Optimization of continual production of CNTs by CVD method using radial basic function (RBF) neural network and the bees algorithm. J Nanostructures 2018; 8: 225–231.
24. Hsieh C-T, Teng H, Chen W-Y, Cheng Y-S. Synthesis, characterization, and electrochemical capacitance of amino-functionalized carbon nanotube/carbon paper electrodes. Carbon. 2010;48(15):4219-29.
25. Li Y, Huang Y, Zhang Z, Duan D, Hao X, Liu S. Preparation and structural evolution of well aligned-carbon nanotube arrays onto conductive carbon-black layer/carbon paper substrate with enhanced discharge capacity for Li–air batteries. Chemical Engineering Journal. 2016;283:911-21.
26. Xie Z, Chen G, Yu X, Hou M, Shao Z, Hong S, et al. Carbon nanotubes grown in situ on carbon paper as a microporous layer for proton exchange membrane fuel cells. International Journal of Hydrogen Energy. 2015;40(29):8958-65.
27. Chen H-C, Wang Y-C, Huang K-T. Selective synthesis of carbon-nanotubes/graphite or carbon-nanotubes/multi-graphene composites on 3-D nickel foam prepared with different nickel catalyst and pre-treatment. Synthetic Metals. 2016;219:124-34.
28. Chen C-C, Chen CF, Hsu C-H, Li IH. Growth and characteristics of carbon nanotubes on carbon cloth as electrodes. Diamond and Related Materials. 2005;14(3-7):770-3.
29. Chen J, Minett AI, Liu Y, Lynam C, Sherrell P, Wang C, et al. Direct Growth of Flexible Carbon Nanotube Electrodes. Advanced Materials. 2008;20(3):566-70.
30. Wang C, Waje M, Wang X, Tang JM, Haddon RC, Yan. Proton Exchange Membrane Fuel Cells with Carbon Nanotube Based Electrodes. Nano Letters. 2004;4(2):345-8.
31. Zhao T, Kvande I, Yu Y, Ronning M, Holmen A, Chen D. Synthesis of Platelet Carbon Nanofiber/Carbon Felt Composite on in Situ Generated Ni−Cu Nanoparticles. The Journal of Physical Chemistry C. 2010;115(4):1123-33.
32. Sun X, Stansfield B, Dodelet JP, Désilets S. Growth of carbon nanotubes on carbon paper by Ohmically heating silane-dispersed catalytic sites. Chemical Physics Letters. 2002;363(5-6):415-21.
33. Chen LH, AuBuchon JF, Chen IC, Daraio C, Ye XR, Gapin A, et al. Growth of aligned carbon nanotubes on carbon microfibers by dc plasma-enhanced chemical vapor deposition. Applied Physics Letters. 2006;88(3):033103.
34. Zhang Q, Liu J, Sager R, Dai L, Baur J. Hierarchical composites of carbon nanotubes on carbon fiber: Influence of growth condition on fiber tensile properties. Composites Science and Technology. 2009;69(5):594-601.
35. Li X, Tuo Y, Jiang H, Duan X, Yu X, Li P. Engineering Pt/carbon-nanofibers/carbon-paper composite towards highly efficient catalyst for hydrogen evolution from liquid organic hydride. International Journal of Hydrogen Energy. 2015;40(36):12217-26.
36. Tuo Y, Jiang H, Li X, Shi L, Yu X, Li P. Kinetic behavior of Pt catalyst supported on structured carbon nanofiber bed during hydrogen releasing from decalin. International Journal of Hydrogen Energy. 2016;41(25):10755-65.
37. Sharma SP, Lakkad SC. Morphology study of carbon nanospecies grown on carbon fibers by thermal CVD

technique. Surface and Coatings Technology. 2009;203(10-11):1329-35.
38. Dresselhaus MS, Jorio A, Hofmann M, Dresselhaus G, Saito R. Perspectives on Carbon Nanotubes and Graphene Raman Spectroscopy. Nano Letters. 2010;10(3):751-8.
39. Hodkiewicz J, Scientific TF. Characterizing Carbon Materials with Raman Spectroscopy. Progress in Materials Science 2005; 50: 929–961.
40. Melanitis N, Tetlow PL, Galiotis C. Characterization of PAN-based carbon fibres with laser Raman spectroscopy. Journal of Materials Science. 1996;31(4):851-60.
41. Chen J, Wang JZ, Minett AI, Liu Y, Lynam C, Liu H, et al. Carbon nanotube network modified carbon fibre paper for Li-ion batteries. Energy & Environmental Science. 2009;2(4):393.
42. Kim C-d, Lee H-R, Kim HT. Effect of NH3 gas ratio on the formation of nitrogen-doped carbon nanotubes using thermal chemical vapor deposition. Materials Chemistry and Physics. 2016;183:315-9.
43. Hsieh C-T, Chen W-Y, Wu F-L. Fabrication and superhydrophobicity of fluorinated carbon fabrics with micro/nanoscaled two-tier roughness. Carbon. 2008;46(9):1218-24.
44. Mohammad Raei Nayini M, Bastani S, Ranjbar Z. Synthesis and characterization of functionalized carbon nanotubes with different wetting behaviors and their influence on the wetting properties of carbon nanotubes/polymethylmethacrylate coatings. Progress in Organic Coatings. 2014;77(6):1007-14.
45. Hsieh C-T, Chen W-Y. Water/oil repellency and drop sliding behavior on carbon nanotubes/carbon paper composite surfaces. Carbon. 2010;48(3):612-9.
46. Hsieh C-T, Chen W-Y, Wu F-L, Hung W-M. Superhydrophobicity of a three-tier roughened texture of microscale carbon fabrics decorated with silica spheres and carbon nanotubes. Diamond and Related Materials. 2010;19(1):26-30.
47. Jiang Y, Lin L. A two-stage, self-aligned vertical densification process for as-grown CNT forests in supercapacitor applications. Sensors and Actuators A: Physical. 2012;188:261-7.
48. Yahya MA, C. W. Ngah CWZ, Hashim MA, Ahmad M, Yarmo MA. Desiccated Coconut Residue Based Activated Carbon as an Electrode Material for Electric Double Layer Capacitor. Applied Physics Research. 2015;7(2).
49. Kim Y-T, Ito Y, Tadai K, Mitani T, Kim U-S, Kim H-S, et al. Drastic change of electric double layer capacitance by surface functionalization of carbon nanotubes. Applied Physics Letters. 2005;87(23):234106.
50. Li J, Cheng X, Shashurin A, Keidar M. Review of Electrochemical Capacitors Based on Carbon Nanotubes and Graphene. Graphene. 2012;01(01):1-13.
51. Wang C-H, Shih H-C, Tsai Y-T, Du H-Y, Chen L-C, Chen K-H. High methanol oxidation activity of electrocatalysts supported by directly grown nitrogen-containing carbon nanotubes on carbon cloth. Electrochimica Acta. 2006;52(4):1612-7.
52. Awitdrus, Deraman M, Talib IA, Farma R, Omar R, Ishak MM, et al. Physical and electrochemical properties of supercapacitor composite electrodes prepared from biomass carbon and carbon from green petroleum coke. AIP Publishing LLC; 2015.
53. Maletin Y, Strelko V, Stryzhakova N, Zelinsky S, Rozhenko AB, Gromadsky D, et al. Carbon Based Electrochemical Double Layer Capacitors of Low Internal Resistance. Energy and Environment Research. 2013;3(2).